

Spatial extension of excitons in triphenylene based polymers given by range-separated functionals

B. Kociper and T.A. Niehaus*

Department of Theoretical Physics, University of Regensburg, 93040 Regensburg,
Germany

ABSTRACT

Motivated by an experiment in which the singlet-triplet gap in triphenylene based copolymers was effectively tuned, we used time dependent density functional theory (TDDFT) to reproduce the main results. By means of conventional and long-range corrected exchange correlation functionals, the luminescence energies and the exciton localization were calculated for a triphenylene homopolymer and several different copolymers. The phosphorescence energy of the pure triphenylene chain is predicted accurately by means of the optimally tuned long-range corrected LC-PBE functional and slightly less accurate by the global hybrid B3LYP. However, the experimentally observed fixed phosphorescence energy could not be reproduced because the localization pattern is different to the expectations: Instead of localizing on the triphenylene moiety - which is present in all types of polymers - the triplet state localizes on the different bridging units in the TDDFT calculations. This leads to different triplet emission energies for each type of polymer. Yet, there are clear indications that long-range corrected TDDFT has the potential to predict the triplet emission energies as well as the localization behavior more accurate than conventional local or semi-local functionals.

1. INTRODUCTION

Today, conjugated polymers play an important role in applications like organic light emitting diodes (OLEDs)¹ or in organic photovoltaics.^{2,3} A key quantity for optimal device performance is the singlet-triplet gap (ΔE_{ST}), because a small gap favours a higher emitter efficiency.⁴ Usually electrical injection of charges into an OLED leads to the generation of singlet and triplet excitations, where the decay of the latter is mostly non-radiative. To promote radiative triplet recombination, heavy-atom centers are employed to promote spin-orbit coupling, leading to a higher phosphorescence probability.⁵⁻⁹ An exception are triphenylene and some other polycyclic aromatic hydrocarbons: The phosphorescence from the triplet state is observed at low temperatures without incorporation of heavy

*Corresponding author: thomas.niehaus@physik.uni-r.de

atoms.^{10–12} A small ΔE_{ST} does not only increase the rate for triplet emission directly,⁹ it allows also for thermal repopulation of the lowest singlet state (S_1), and a following delayed fluorescence. This *singlet harvesting* approach was recently put forward by Yersin and co-workers to enable the collection of both singlet and triplet excitons that are created by charge injection in OLED.^{13,14}

In a recent experiment,¹⁵ the group of Lupton investigated the singlet-triplet splitting in a series of triphenylene based phosphorescent copolymers and showed that ΔE_{ST} may be effectively tuned (see Figure 1). The copolymers exhibit all a similar triplet spectrum at the same energetic position, whereas the energy of the singlet peak strongly depends on the details of the polymer backbone. The fact that the singlet emission shifts towards the triplet emission from monomer **1** to polymer **6**, whereas the triplet level remains almost unchanged, implies that singlet and triplet excitations can form on different parts of the conjugated system.¹⁶ This indicates that the splitting can be tuned and that eventually even the regular level ordering of singlet and triplet may be inverted.¹⁵

Our goal in this study is to investigate whether time dependent density functional theory (TDDFT) with state of the art exchange correlation (xc) functionals is capable of describing this highly unusual photo-chemical system. The interest arises, because popular local and semi-local xc functionals that are widely used for condensed matter applications fail to provide a reasonable description of the electronic structure in extended π -conjugated systems. Typical shortcomings for polymers are an underestimated bond length alternation,^{17,18} an overestimation of electronic polarizabilities¹⁹ and conductances,²⁰ the instability of polaronic excitations,²¹ and an underestimation of the optical gap. Many of these deficiencies have been related to the incomplete cancellation of self-interaction effects due to approximate exchange functionals which lead to an overly delocalized electron density.²² To a large extent these difficulties may be overcome by range-separated xc functionals, that recently achieved a lot of attention. The main idea is to separate the electron-electron interaction into a short-range domain, where conventional semi-local functionals work well, and a long-range domain, where non-local Hartree-Fock (HF) exchange reduces self-interaction errors significantly.^{23,24} In the early formulations,^{25,26} the domains were defined by a single empirical parameter valid for all systems. Following the work of Baer and coworkers²⁷ this parameter may also be tuned on a system per system basis to match known conditions for the exact functional (e.g., the ionization potential being equal to the highest occupied orbital energy), escaping the need for an empirical fit to a large training set of molecules. Earlier studies indicate the importance of non-local exchange (either within conventional global hybrids or tuned range-separated xc functionals) also for the correct estimation of exciton sizes.^{28–30} As the mentioned experiment focuses on luminescence properties of the triphenylene polymers, we are especially interested in the spatial extension of the lowest singlet and triplet states after excited state relaxation has taken place.

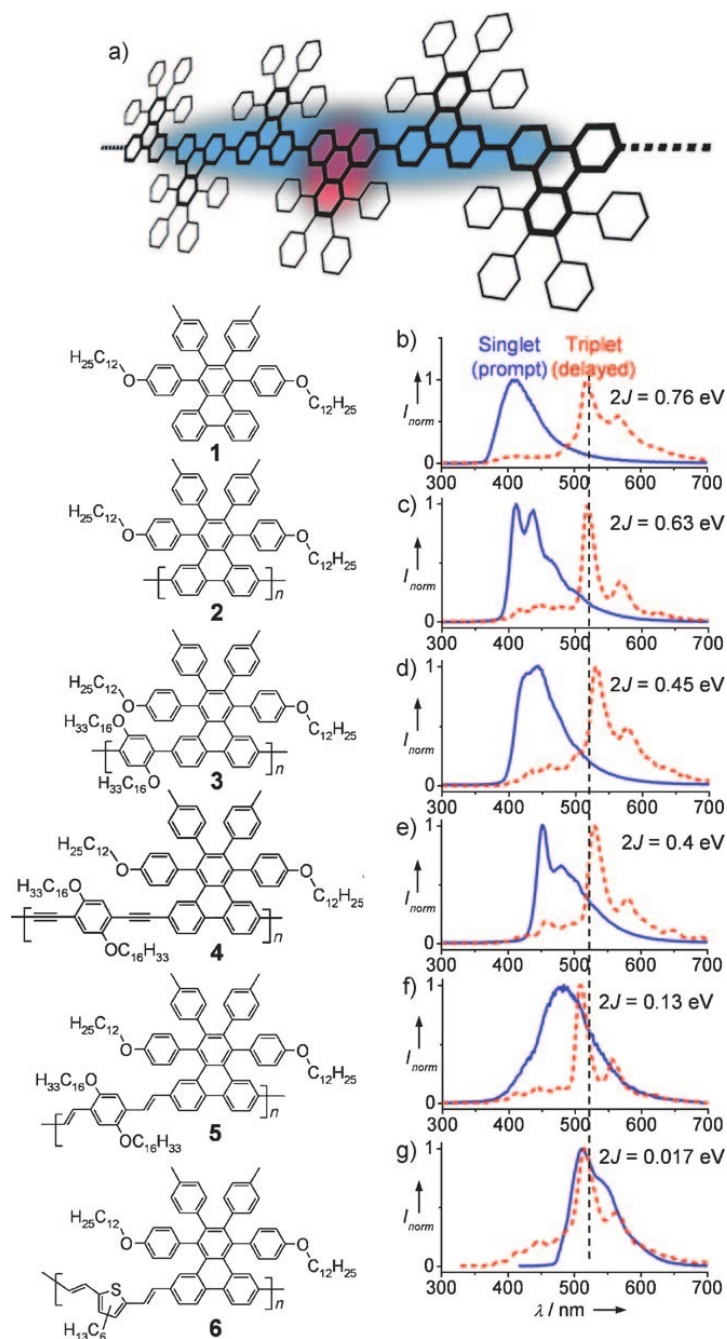


Figure 1: Fluorescence (prompt emission) and phosphorescence (delayed emission) from a triphenylene-based monomer and conjugated copolymers, dispersed in a polystyrene matrix at 25 K. a) Delocalization of singlet excitations (blue) with triplets (red) localized at the triphenylene unit. b) - g) Singlet (solid blue line, integrated 0-2 ns after excitation) and triplet (dashed red line) spectra of the monomer **1** (0.1 - 1.1 ms delay after excitation), the homopolymer **2** (9 - 10 ms delay), the para-phenylene copolymer **3** (12 ms delay), the ethynylene copolymer **4** (1.5 - 2.5 ms delay), phenylene vinylene copolymer **5** (0.02 - 1.02 ms delay), and the thienylene vinylene copolymer **6** (0.05 - 5.05 ms delay). The exchange splitting $2J$ is estimated from the peak separations. The dashed black line indicates the average triplet peak position. Reprinted with permission from Ref. [15].

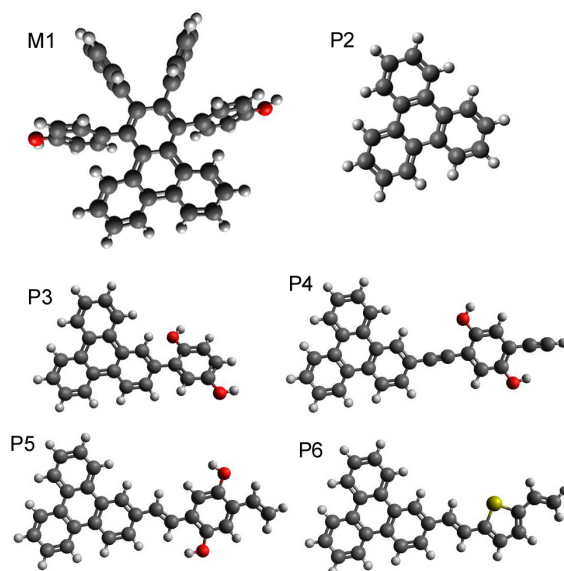


Figure 2: Model structure for the triphenylene based monomer **M1** and basic repeat units of the polymers **P2-P6** used in this study.

2. COMPUTATIONAL DETAILS

In order to build realistic but still numerically tractable models for the copolymers depicted in Figure 1, we removed the toluene and phenol groups bonded to the triphenylene unit and all alkane chains to arrive at the polymer building blocks depicted in Figure 2. Mass spectra from the experiment yield the number of basic units for each polymer. Approximately 48-52 units formed the triphenylene polymer **2**, around 32-34 units the polymer **3**, 15-17 units the polymer **4** and only 5-7 units the polymer **5** and 4-6 units the polymer **6**. As the TDDFT calculations for chains with more than 260 atoms were computationally too demanding, the number of basic units in a chain was limited to $n=6$. Therefore the TDDFT results for polymer **5** and **6** can be directly compared to experiment, whereas the other polymer types **2**, **3**, and **4** could not be calculated up to comparable length scales. In the following, oligomers with n repetitions of the basic unit α are denoted as $\mathbf{P}_{\alpha n}$. We also considered the monomer **1**, which differs from the corresponding structure in the experiment only in the missing alkane chains and methyl groups, which should have a marginal influence on the optical properties. All structures were optimized without symmetry constraints using the hybrid B3LYP³¹ functional and a 6-31G* basis set with the NWChem 6.0 code.³² In contrast to local and semi-local functionals, B3LYP provides more realistic values for the bond length alternation in conjugated polymers, especially for short chains.¹⁷

For the excited state calculations we compare the semi-local PBE functional,³³ the hybrid B3LYP, and the range-separated LC-PBE functional. Range-separated functionals partition the Coulomb

operator into a short-range and long-range component, ruled by the parameter γ , for example by utilizing the standard error-function $\text{erf}(x)$.^{25,26}

$$\frac{1}{r} = \frac{1 - \text{erf}(\gamma r)}{r} + \frac{\text{erf}(\gamma r)}{r}. \quad (1)$$

The first term is a Coulomb operator decaying to zero on a length scale of $\approx 1/\gamma$ and is therefore short-ranged (SR), while the second term dominates at large r accounting for the long-range (LR) behavior. Both conventional pure and hybrid functionals may be extended according to this idea. In the former case the functional decomposition reads

$$E_{xc} = E_{x,\text{DFT}}^{\text{SR}}(\gamma) + E_{x,\text{HF}}^{\text{LR}}(\gamma) + E_{c,\text{DFT}}. \quad (2)$$

In the case of LC-PBE, $E_{x,\text{DFT}}^{\text{SR}}$ is the short-range form of the gradient-corrected PBE exchange functional,³⁴ $E_{x,\text{HF}}^{\text{LR}}$ denotes the Hartree-Fock exchange energy evaluated with the long-range part of the interaction in Equation 1, while the correlation part $E_{c,\text{DFT}}$ is left unchanged with respect to the usual form of PBE. Instead of working with a fixed value of the range-separation parameter γ , we follow the ideas of Baer and co-workers²⁷ to determine its value for each system separately. To this end, one considers the following error function

$$\Delta_{\text{IP}}(\gamma) = |\epsilon_{\text{HOMO}}^{\gamma} - [E_{\text{tot}}^{\gamma}(N) - E_{\text{tot}}^{\gamma}(N - 1)]|, \quad (3)$$

where $\epsilon_{\text{HOMO}}^{\gamma}$ denotes the orbital energy of the highest occupied molecular orbital (HOMO) and $E_{\text{tot}}^{\gamma}(N)$ and $E_{\text{tot}}^{\gamma}(N - 1)$ stand for the total energy of the neutral system with N electrons and the ionized one. The latter is obtained by means of a spin unrestricted calculation. Minimization of Δ_{IP} yields the optimal range-separation parameter and enforces a condition that the exact exchange-correlation functional should exhibit, namely that the negative of the HOMO energy equals the ionization potential. Key to the success of this scheme is the fact that ionization energies obtained from total energy differences are typically quite accurate in DFT.

For the different functionals, vertical excitation energies were obtained from frequency domain TD-DFT in linear response (a.k.a. RPA or Casida approach).³⁵ The Tamm Dancoff approximation³⁶ (TDA) was employed, because there is evidence that this improves the lowest lying singlet and triplet states as explained in the next section. Additionally, the use of the TDA enabled the calculation of longer polymer chains, as the computational effort is reduced. The 6-31G* basis set was used for all excited state computations. Test calculations on the basic triphenylene unit (**P2**₁) with a basis set of triple- ζ quality and polarization functions on all atoms led to a change of only 0.02 eV for S_1 and T_1 excitation energies. This deviation is expected to be much smaller than the error introduced by the molecular models and the available approximate exchange-correlation functionals.

Fluorescence and phosphorescence energies were obtained by optimizing the geometry on the S_1 and T_1 potential energy surface, respectively. At the resulting geometry, vertical emission energies were computed by means of linear response TD-DFT to estimate the energy of maximum emission. Because of the high computational cost, excited state optimization in the singlet state could only be performed for the polymers **P2** and **P6**. The Amsterdam Density Functional program (ADF)^{37–39} with DZP basis set was used for this purpose. Optimization in the T_1 was carried out again with NWChem 6.0 using ground state DFT with a spin multiplicity of three and 6-31G* basis. The geometry of polymer **4** was difficult to converge especially in the triplet state. The corresponding results are incomplete and therefore left out in the following discussion.

3. RESULTS

3.1 Polymer structure

While the polymers were dispersed and embedded in a polystyrene matrix in the experiment, our calculations correspond to single molecules in the gas phase. It is difficult to quantify the influence of the surrounding medium on the polymer structure precisely, but it seems natural to assume that a planarization of the polymer backbone takes place to reduce steric hindrance. Nevertheless, we do not enforce perfect planarity in the optimizations, since recent thin film results indicate inter- and intra-segment twist in a variety of copolymers.^{40–42} Without symmetry constraints, twisted geometries are obtained in the ground state for polymer **2** and **3**, whereas for polymer **5** and **6** planar geometries showed to be energetically favored. For **P2** we additionally tested the impact of forced planar structures on the results. The T_1 absorption and emission energies for the planar compounds lie in average 0.23 eV and 0.13 eV, respectively, below the ones for twisted geometries. Important for the following is that both type of structures exhibited very similar localization characteristics of the excited state.

In order to assess the significance of our reduced molecular models, the absorption and luminescence energies of **M1** and **P2₁** are compared in Table 1. The two compounds differ only in the attached functional groups, which are left out in the longer polymer models. It turns out, that for these monomers the influence of the aromatic substituents is sizable and leads to a red shift (depending on the functional) of 0.2-0.4 eV in absorption and of 0.6 eV in emission. Interestingly, unconstrained optimization of **M1** in the T_1 state led to rotation of the attached benzene moieties and a concomitant closing of the optical gap. Such a volume demanding structural change is not likely in a matrix environment. Therefore, the dihedral angle of the functional groups was fixed with respect to the triphenylene plane and the resulting phosphorescence energies in Table 1 are obtained. All functionals show a reasonable agreement with the experimental result of 2.37 eV given by Lupton.

	Functional	S ₁ absorption			T ₁ absorption		T ₁ emission	
		Energy	f	Φ_i^a	Energy	Φ_i^a	Energy	Φ_i^a
M1	PBE	3.18	0.07	Φ_H^L	2.84	Φ_H^L	1.95	Φ_H^L
	B3LYP	3.76	0.01	$\Phi_H^{L+1}, \Phi_{H-1}^L$	3.02	Φ_H^L	2.05	Φ_H^L
	LC-PBE	3.88	0.01	$\Phi_H^{L+1}, \Phi_{H-1}^L$	3.14	Φ_H^L	2.06	Φ_H^L
P2₁	PBE	3.68	0.00	$\Phi_H^{L+1}, \Phi_{H-1}^L$	3.17	$\Phi_H^L, \Phi_{H-1}^{L+1}$	2.64	Φ_H^L
	B3LYP	4.03	0.00	$\Phi_H^{L+1}, \Phi_{H-1}^L$	3.21	$\Phi_H^L, \Phi_{H-1}^{L+1}$	2.63	Φ_H^L
	LC-PBE	4.29	0.00	$\Phi_H^{L+1}, \Phi_{H-1}^L$	3.36	$\Phi_H^L, \Phi_{H-1}^{L+1}$	2.77	Φ_H^L

Table 1: S₁/T₁ absorption and T₁ emission energies (in eV) for the monomer **M1** and **P2₁** (i.e. Triphenylene). Oscillator strengths (f) are given for singlet-singlet transitions only. Singly excited determinants that contribute significantly to the excited state wave function are denoted as Φ_i^a (for a transition from orbital i to a). The highest occupied molecular orbital (HOMO) is abbreviated as H , the lowest unoccupied one (LUMO) as L . The range-separation parameter was determined to be $\gamma = 0.17 \text{ a}_0^{-1}$ for **M1** and $\gamma = 0.23 \text{ a}_0^{-1}$ for **P2₁**. The experimental T₁ emission energy for **M1** is 2.37 eV,¹⁵ and the S₁ absorption energy for triphenylene in solution was reported to be 3.78 eV.⁴³

For triphenylene, the S₀ → S₁ transition is symmetry forbidden, and is allowed but very weak for **M1**. This indicates that the additional functional groups perturb and influence the electronic structure, but do not completely change it. Further evidence for this fact is given by the spatial extension of the frontier molecular orbitals for longer oligomers depicted in Figure 3. These are located mainly on the inner triphenylene rings along the chain direction. Compared to the non-negligible effect for the monomer, additionally attached benzene units may hence play a less important role in the polymer limit. It should also be mentioned at this point, that the frontier orbitals are delocalized over the full chain. The excited state localization schematically depicted in Figure 1a is not present in absorption.

3.2 Ordering of the two lowest singlet excited states

Special attention was paid to the two lowest singlet excited states. One of these, which is commonly denoted with L_a is mainly a HOMO → LUMO excitation. The other one, L_b , consists by more or less equal parts of the HOMO-1 → LUMO and HOMO → LUMO+1 transition. For linear acenes as well as triphenylene and also some nonlinear PAHs (polycyclic aromatic hydrocarbons), the L_a is stated to have charge-transfer (CT) character, whereas the L_b is covalent like the ground state.^{44, 45} To find out whether one of the first excited states is charge-transfer like is important, because it is well known,^{46–48} that TDDFT predicts those energies with large errors increasing with system size.⁴⁹

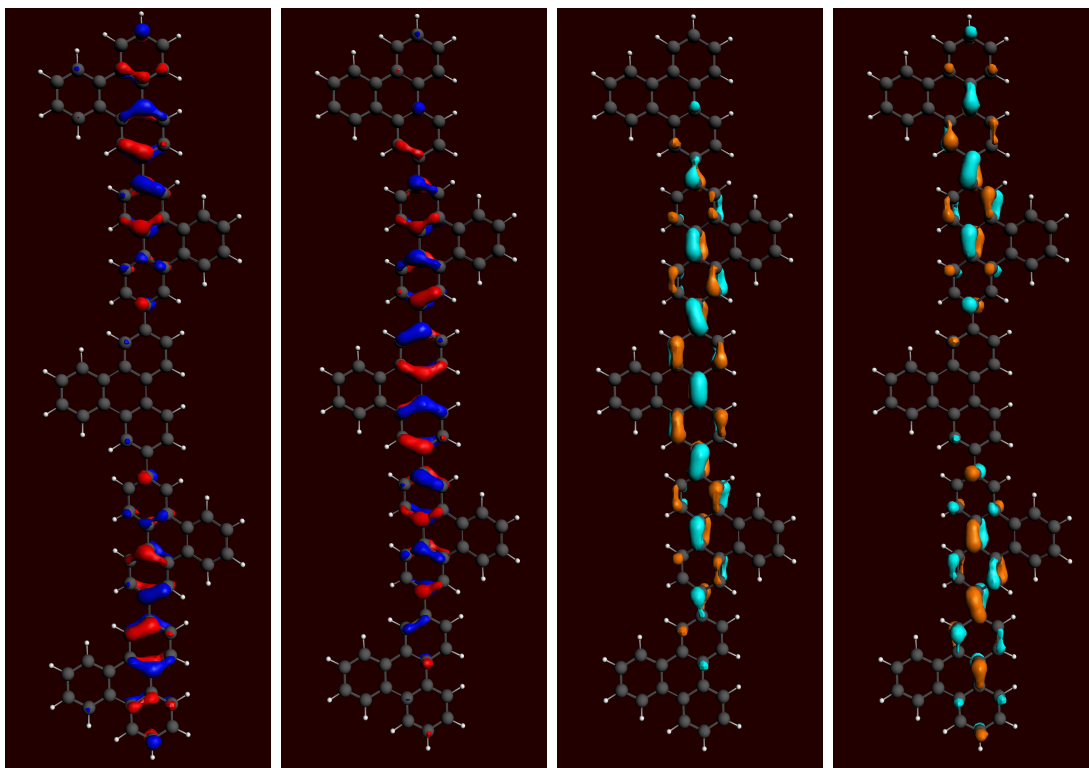


Figure 3: From left to right: molecular orbitals HOMO-1, HOMO, LUMO and LUMO+1 of **P2₅** at the B3LYP/DZP level of theory.

Several studies have shown,^{50–52} that range-separated functionals decrease this error for CT states; in some cases even its system size dependence.⁵² Some care is necessary in the evaluation of triplet states as they can be sensitive to instabilities in the ground state⁵³ – but this may be cured by a system dependent determination of the range separation parameter γ plus the TDA,⁵⁴ which is also favorable because it reduces memory requirements.

The calculations of all polymers show that the investigated chains generally do not show a wrong ordering of the two lowest singlet excited states. Only one molecule, **P2₃**, switches its lowest lying singlet states when using the LC-PBE functional instead of B3LYP or PBE. Since fluorescence is strong in the experiment, one expects the S_1 to be strongly dipole allowed. This is also found in the calculations, where (apart from the shorter **P2₂** and **P3₁**) the S_1 is dominated by the HOMO \rightarrow LUMO transition and exhibits a sizable oscillator strength that increases linearly with chain length for the B3LYP and LC-PBE functionals.

3.3 Scaling of the range separation parameter

If obtained from a tuning criterion like Equation 3, the parameter γ determines the optimal range of a local description of exchange effects by means of conventional Kohn-Sham DFT. It should

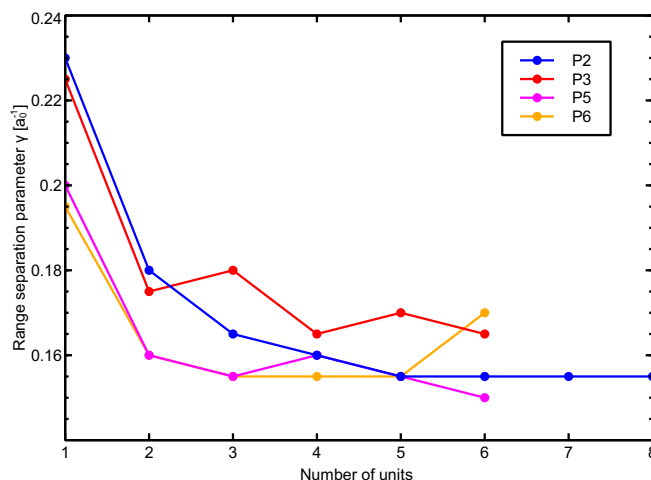


Figure 4: Optimal range separation parameter in units of the inverse Bohr radius (a_0) versus number of polymer units. The minimum of Δ_{IP} was found by varying γ in increments of $0.005 a_0^{-1}$.

therefore depend on the actual electronic structure of the system of interest, which is encoded in system specific variables like the electron density or microscopic dielectric function. A recent investigation indicates a close correlation of the range separation parameter with the conjugation length in polymers.^{30,55} For alkanes and polythiophenes a clear saturation of $1/\gamma$ with system size was observed, in full agreement with a finite conjugation length. In contrast, this parameter increased linearly for oligoacenes up to nine benzene rings.⁵⁵ The results depicted in Figure 4 confirm a saturation of γ , which is most clearly seen for **P2**. The range separation parameter depends strongly on the chemical structure of the copolymer and seems to converge for $n > 4$ to values between $0.15 a_0^{-1}$ and $0.17 a_0^{-1}$. The optimal range separation parameter therefore decreases with system size, but it does not tend to zero. This means that the tuned LC-PBE functional differs from PBE also in the polymer limit.

3.4 Transition energies

We now move to central part of the present investigation, the electronic excited states. Figure 5 shows the triplet absorption and emission energies as a function of the oligomer length. As expected from a simple particle-in-a-box model, the excited state energies decrease with increasing length of the π -conjugated system. The decrease is steeper for the local PBE functional in comparison to the two functionals that involve a part of HF-exchange. This was already noted by Gierschner et al.⁵⁶ and can be traced back to the structure of the RPA equations in TDDFT, as we believe. Corrections to Kohn-Sham single-particle excitations are brought about by the so-called coupling matrix, which features exchange-like two-electron integrals for pure functionals.³⁵ These tend to zero for extended molecular orbitals, such that the excited state energies given by TDDFT reduce to simple molecular

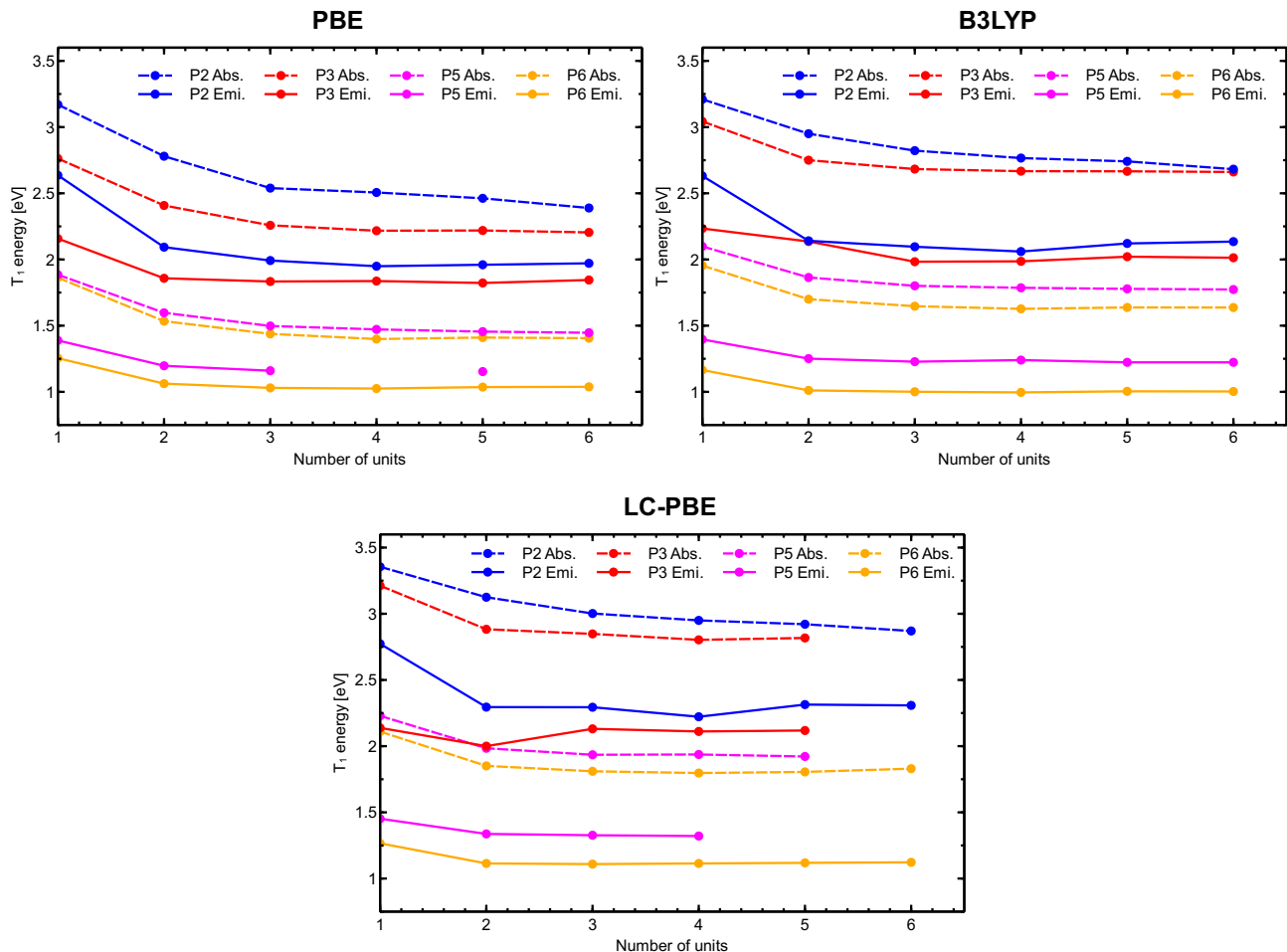


Figure 5: T_1 absorption and emission energies with increasing polymer length at the PBE, B3LYP and LC-PBE level. Missing datapoints correspond to unconverged calculations. The triplet emission energy depends on the type of polymer, whereas experimentally¹⁵ the triplet phosphorescence is measured at an almost fixed value of 2.37 eV for *each* copolymer.

orbital energy differences. Within a particle-in-a-box model the latter scale as $1/L^2$, where L denotes the effective conjugation length. In contrast, the coupling matrix involves Coulomb-like two-electron integrals with $1/L$ scaling for functionals that involve HF-exchange.⁵⁷

With respect to convergence to the polymer limit, the T_1 energies of all copolymers saturate with some fluctuations after approximately four repeat units. Compared to scaling of the range separation parameter, the convergence occurs faster here. A further observation is related to the absolute size of the triplet excitation energies, which follow the order LC-PBE > B3LYP > PBE in line with the extensive benchmark provided by Jacquemin et al.⁵³ This study indicates an underestimation of T_1 energies of roughly 0.4 eV with respect to theoretical best estimates for the present functionals.

For the longest calculated triphenylene chain **P2₆**, the LC-PBE functional delivers a phosphorescence energy of 2.31 eV and comes very close to the experimental result of 2.39 eV given by Lupton. In stark disagreement with the measurements, the different copolymers do however not converge to the same emission energy. The large Stokes shift of 0.5 eV, on average, points towards a significant excited state relaxation and concomitant change of excited state nature.

3.5 Localization behavior

In order to quantify these geometrical changes, we follow Ref. [49] and plot the bond length difference between S_0 and T_1 optimized geometries along the central carbon chain in Figure 6. Generally the bonding pattern changes from aromatic to quinoid form. Focusing first on the pure triphenylene polymer **P2** (Figure 6a), we find in agreement with the experimental results, that the structural changes are localized on one of the triphenylene units for B3LYP and LC-PBE. In contrast, PBE predicts bond length changes that are smeared out over the full chain. As already mentioned in the introduction, this delocalization error can be traced back to spurious self-interaction in the local PBE functional.

For **P3** in Figure 6b, a similar behavior is found for the PBE functional. The hybrid B3LYP favors again a localization, but this time not on the triphenylene moiety of the copolymer, but on the benzoquinone. Also for **P5**, both B3LYP and LC-PBE predict a localization on the bridging units, although they differ in the actual unit along the chain. The localization pattern for **P6** follows this trend, again the excited state is predominantly localized on the bridging unit thiophene for B3LYP and LC-PBE, while the PBE result is fully delocalized. Interestingly, a partial localization on a triphenylene unit is observed for the B3LYP functional for this polymer.

The discrepancy between theory and experiment mentioned in the last section can now be explained. The calculations predict either a localization on a different moiety of the polymer as the experiment (B3LYP, LC-PBE), or no localization at all (PBE). Since the localization occurs on different chemical units for the different polymers, also the phosphorescence energies must vary in contrast to the experimental results which indicate exclusively triphenylene emission. In line with this, the LC-PBE results are in good quantitative agreement for the pure triphenylene polymer **P2** only.

Although the optimizations in the first singlet state could only be performed for a subset of all polymers and functionals, we shortly discuss **P6** as an example. Figure 7 depicts a comparison of S_1 and T_1 bond length differences with respect to the ground state. It is obvious, that the triplet excited state is more localized than the singlet excited state, which also agrees with the experimental findings. This can be rationalized by the fact, that the triplet state is stabilized against the singlet due

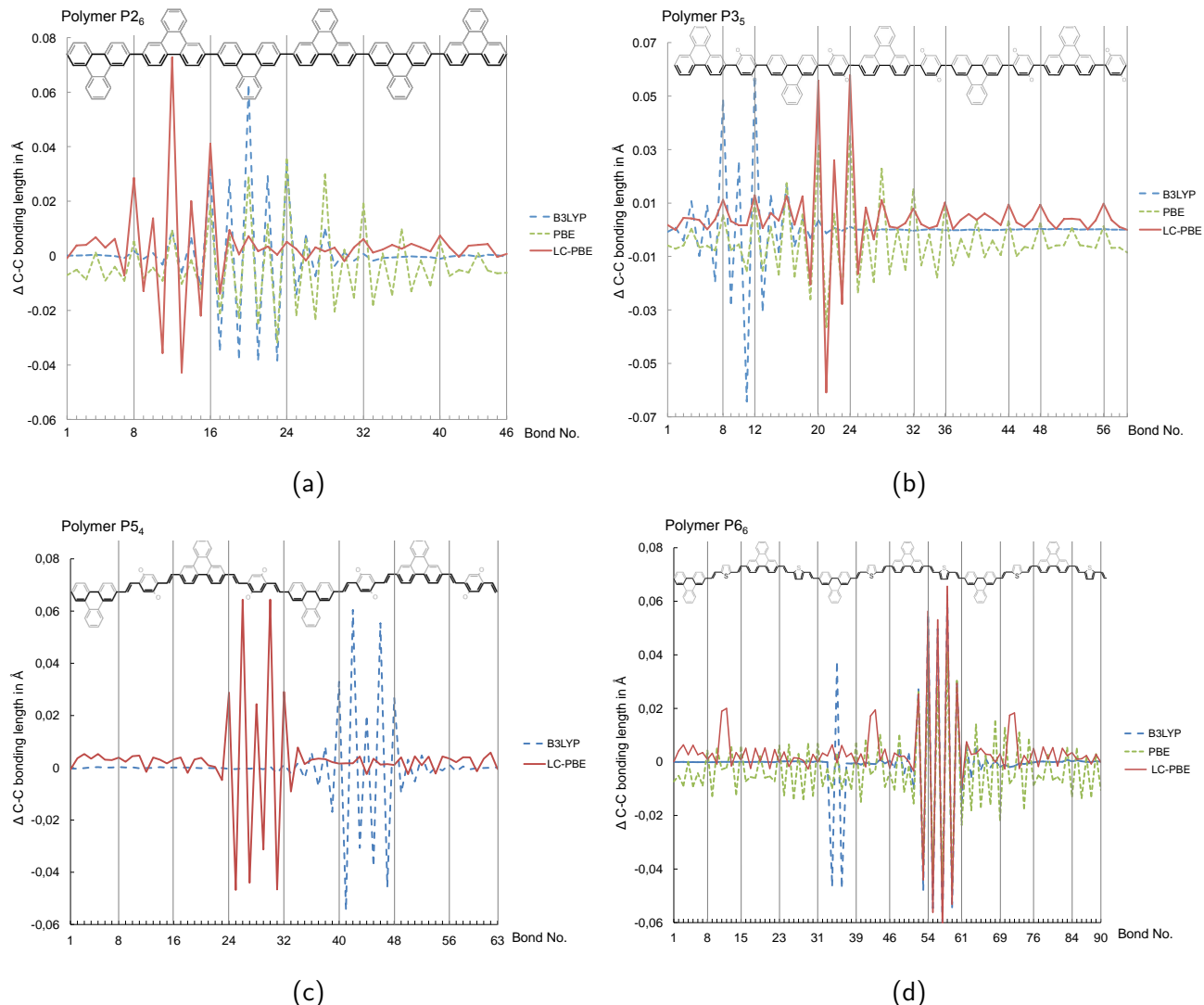


Figure 6: C-C bond length difference between geometries optimized in the S_0 and T_1 state along the sketched path for the different polymers. The difference shows where bonds get tighter (positive value) or looser (negative value).

to the attractive exchange interaction between electrons. The latter is maximized by wave function localization, which promotes a structural change towards a confined exciton.

4. CONCLUSIONS

The results of the present study create mixed impressions. Some aspects of the experiment are well reproduced, while others call for further improvement of the computational methodology. On the positive side, a central point of the experiment was the hypothesis that *singlet and triplet excitations*

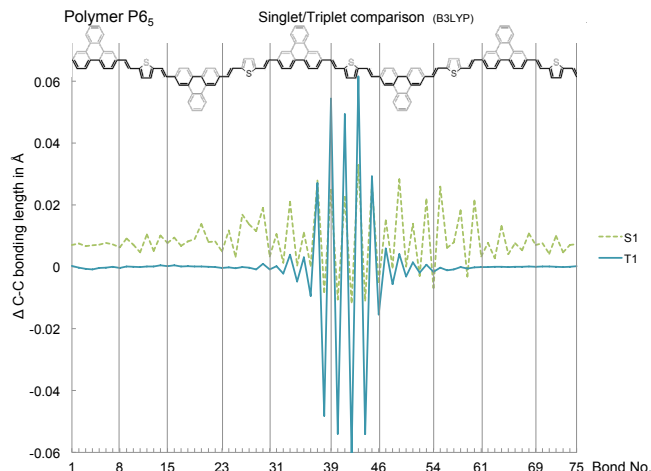


Figure 7: S_0/S_1 as well as S_0/T_1 bond length difference for **P6₅** at the B3LYP level

can form on different parts of the of the conjugated system,¹⁵ which eventually allowed the singlet-triplet gap to be tuned. The calculations confirm this and show explicitly that the localization is not present in absorption, but instead driven by geometrical relaxation in the excited state. The simulations describe also the different extension of triplet and singlet excitons qualitatively correct and reach quantitative accuracy for the phosphorescence energy of the pure triphenylene polymer.

On the negative side, none of the employed functionals was able to reproduce the triplet emission at fixed energy. No clear advantage of tuned range-separated over hybrid functionals can be ascertained in this respect, although the absolute values for triplet emission energies are bit more accurate for the former. It became also clear, that local functionals like PBE are not the optimal choice for extended π -conjugated systems. Besides their known deficiencies for these systems, like an underestimated bond length alternation and underestimated vertical excitation energies, we also found an erroneous excited state relaxation in this study. The reduced self-interaction error in hybrid and range separated functionals helps to diminish this problem. There is still room for improvement, since tuned range-separated functionals violate size consistency while hybrid functionals suffer from remaining self interaction.¹⁸

Besides deficiencies in the available functionals, there are also other possible reasons for the remaining discrepancies between theory and experiment. The first one is related to the observation that the optimization in the triplet state locates only the local minimum that is nearest to the Franck-Condon point. The fact that LC-PBE and B3LYP show a localization on the same chemical group, but on different units along the chain, hints at several minima on the T_1 potential energy surface. The underlying physical picture is that of a polymer as a multi-chromophoric system,⁴¹ where excitons can relocate between different chemical units by means of Förster energy transfer. In principle, this could

be tested with excited state molecular dynamics simulations, which are unfortunately prohibitively expensive for the polymers under study. A related point concerns the simplified model structures we employed in this work. In section 3.1 we argued against a major influence of the aromatic groups that are attached to the triphenylene moieties. Notwithstanding, the small red-shift they induce might be sufficient to stabilize the exciton on this moiety. Further experimental studies on unfunctionalized triphenylene polymers could shed further light on this question and help in the validation of current computational approaches.

5. ACKNOWLEDGMENTS

The authors would like to thank John Lupton for fruitful discussions. Financial support from the Deutsche Forschungsgemeinschaft (GRK 1570 and SPP 1243) is also gratefully acknowledged.

REFERENCES

1. A. Grimsdale, K. Chan, R. Martin, P. Jokisz, and A. Holmes, "Synthesis of light-emitting conjugated polymers for applications in electroluminescent devices," *Chem. Rev.*, vol. 109, pp. 897–1091, 2009.
2. C. Brabec, V. Dyakonov, J. Parisi, and N. Sariciftci, *Organic Photovoltaics: Concepts and Realization*. Springer Series in Materials Science, 2003.
3. S. Günes, H. Neugebauer, and N. S. Sariciftci, "Conjugated polymer-based organic solar cells," *Chem. Rev.*, vol. 107, pp. 1324–1338, 2007.
4. B. Milián-Medina and J. Gierschner, *Organic Electronics*, vol. 13. Elsevier B.V., 2012.
5. M. Baldo, D. O'Brien, Y. You, A. Shoustikov, S. Sibley, M. Thompson, and S. Forrest, "Highly efficient phosphorescent emission from organic electroluminescent devices," *Nature*, vol. 395, p. 151, 1998.
6. V. Cleave, G. Yahiolu, P. Le Barny, R. Friend, and N. Tessler, "Harvesting singlet and triplet energy in polymer leds," *Adv. Mat.*, vol. 11, p. 285, 1999.
7. X. Yang, D. Müller, D. Neher, and K. Meerholz, "Highly efficient polymeric electrophosphorescent diodes," *Adv. Mater.*, vol. 18, p. 948, 2006.
8. L. Ying, A. Zhang, W. Yang, and Y. Cao, "Electrophosphorescent light-emitting polymers," *Prog. Chem.*, vol. 21, p. 1275, 2009.
9. S. Haneder, E. Da Como, J. Feldmann, J. M. Lupton, C. Lennartz, P. Erk, E. Fuchs, O. Molt, I. Münster, C. Schildknecht, *et al.*, "Controlling the radiative rate of deep-blue electrophosphorescent organometallic complexes by singlet-triplet gap engineering," *Adv. Mat.*, vol. 20, no. 17, pp. 3325–3330, 2008.
10. W. Clark, A. D. Litt, and C. Steel, "Triplet lifetimes of benzophenone, acetophenone, and triphenylene in hydrocarbons," *J. Am. Chem. Soc.*, vol. 91, no. 19, pp. 5413–5415, 1969.

11. R. Kellogg and R. Bennett, "Radiationless intermolecular energy transfer. iii. determination of phosphorescence efficiencies," *J. Chem. Phys.*, vol. 41, p. 3042, 1964.
12. J. Langelaar, R. Rettschnick, A. Lambooy, and G. Hoytink, "Monomer and excimer phosphorescence of phenanthrene and naphthalene in solution," *Chem. Phys. Lett.*, vol. 1, no. 12, pp. 609–612, 1968.
13. R. Czerwieniec, J. Yu, and H. Yersin, "Blue-light emission of cu (i) complexes and singlet harvesting," *Inorg. Chem.*, vol. 50, no. 17, pp. 8293–8301, 2011.
14. H. Yersin, A. F. Rausch, R. Czerwieniec, T. Hofbeck, and T. Fischer, "The triplet state of organo-transition metal compounds. triplet harvesting and singlet harvesting for efficient oleds," *Coord. Chem. Rev.*, vol. 255, no. 21, pp. 2622–2652, 2011.
15. D. Chaudhuri, H. Wettach, K. van Schooten, S. Liu, E. Sigmund, S. Höger, and J. Lupton, "Tuning the singlet-triplet gap in metal-free phosphorescent π -conjugated polymers," *Angew. Chem. Int.*, vol. 49, p. 7714, 2010.
16. K. Glusac, M. E. Köse, H. Jiang, and K. S. Schanze, "Triplet excited state in platinum-acetylide oligomers: Triplet localization and effects of conformation," *J. Phys. Chem. B*, vol. 111, no. 5, pp. 929–940, 2007.
17. D. Jacquemin and C. Adamo, "Bond length alternation of conjugated oligomers: wave function and dft benchmarks," *J. Chem. Theory Comput.*, vol. 7, no. 2, pp. 369–376, 2010.
18. T. Körzdörfer, R. M. Parrish, J. S. Sears, C. D. Sherrill, and J.-L. Brédas, "On the relationship between bond-length alternation and many-electron self-interaction error," *J. Chem. Phys.*, vol. 137, p. 124305, 2012.
19. B. Champagne, E. A. Perpete, D. Jacquemin, S. J. van Gisbergen, E.-J. Baerends, C. Soubra-Ghaoui, K. A. Robins, and B. Kirtman, "Assessment of conventional density functional schemes for computing the dipole moment and (hyper) polarizabilities of push-pull π -conjugated systems," *J. Phys. Chem. A*, vol. 104, no. 20, pp. 4755–4763, 2000.
20. S. H. Ke, H. U. Baranger, and W. Yang, "Role of the exchange-correlation potential in ab initio electron transport calculations," *J. Chem. Phys.*, vol. 126, p. 201102, 2007.
21. T. A. Niehaus, A. Di Carlo, and T. Frauenheim, "Effect of self-consistency and electron correlation on the spatial extension of bipolaronic defects," *Org. Elec.*, vol. 5, p. 167, June 2004.
22. A. J. Cohen, P. Mori-Sanchez, and W. Yang, "Insights into current limitations of density functional theory," *Science*, vol. 321, p. 792, 2008.
23. P. Mori-Sánchez, A. J. Cohen, and W. Yang, "Many-electron self-interaction error in approximate density functionals," *J. Chem. Phys.*, vol. 125, p. 201102, 2006.
24. R. Haunschild, T. M. Henderson, C. A. Jiménez-Hoyos, and G. E. Scuseria, "Many-electron self-interaction and spin polarization errors in local hybrid density functionals," *J. Chem. Phys.*, vol. 133, p. 134116, 2010.

25. P. M. W. Gill, R. D. Adamson, and J. A. Pople, "Coulomb-attenuated exchange energy density functionals," *Mol. Phys.*, vol. 88, p. 1005, 1996.
26. A. Savin, *Recent developments and applications of modern density functional theory*, pp. 327–357. Elsevier, 1996.
27. R. Baer, E. Livshits, and U. Salzner, "Tuned range-separated hybrids in density functional theory," *Annu. Rev. Phys. Chem.*, vol. 61, pp. 85–109, 2010.
28. S. Tretiak, K. Igumenshchev, and V. Chernyak, "Exciton sizes of conducting polymers predicted by time-dependent density functional theory," *Phys. Rev. B*, vol. 71, no. 3, p. 033201, 2005.
29. I. H. Nayyar, E. R. Batista, S. Tretiak, A. Saxena, D. Smith, and R. L. Martin, "Localization of electronic excitations in conjugated polymers studied by dft," *J. Phys. Chem. Lett.*, vol. 2, no. 6, pp. 566–571, 2011.
30. L. Pandey, C. Doiron, J. S. Sears, and J.-L. Brédas, "Lowest excited states and optical absorption spectra of donor–acceptor copolymers for organic photovoltaics: a new picture emerging from tuned long-range corrected density functionals," *Phys. Chem. Chem. Phys.*, vol. 14, no. 41, pp. 14243–14248, 2012.
31. A. D. Becke, "Density-functional thermochemistry. iii. the role of exact exchange," *J. Chem. Phys.*, vol. 98, p. 5648, 1993.
32. M. Valiev, E. J. Bylaska, N. Govind, K. Kowalski, T. P. Straatsma, H. J. Van Dam, D. Wang, J. Nieplocha, E. Apra, T. L. Windus, and W. A. de Jong, "Nwchem: a comprehensive and scalable open-source solution for large scale molecular simulations," *Comput. Phys. Commun.*, vol. 181, no. 9, pp. 1477–1489, 2010.
33. J. Perdew, K. Burke, and M. Ernzerhof, "Generalized gradient approximation made simple," *Phys. Rev. Lett.*, vol. 77, no. 18, pp. 3865–3868, 1996.
34. T. Yanai, D. P. Tew, and N. C. Handy, "A new hybrid exchange–correlation functional using the coulomb-attenuating method (cam-b3lyp)," *Chem. Phys. Lett.*, vol. 393, no. 1, pp. 51–57, 2004.
35. M. E. Casida, *Recent Advances in Density Functional Methods, Part I*, ch. Time-dependent Density Functional Response Theory for Molecules, pp. 155–192. World Scientific, 1995.
36. S. Hirata and M. Head-Gordon, "Time-dependent density functional theory within the tamm–dancoff approximation," *Chem. Phys. Lett.*, vol. 314, no. 3, pp. 291–299, 1999.
37. G. Te Velde, F. M. Bickelhaupt, E. J. Baerends, C. Fonseca Guerra, S. J. van Gisbergen, J. G. Snijders, and T. Ziegler, "Chemistry with adf," *J. Comput. Chem.*, vol. 22, no. 9, pp. 931–967, 2001.
38. C. F. Guerra, J. Snijders, G. Te Velde, and E. Baerends, "Towards an order-n dft method," *Theor. Chem. Acc.*, vol. 99, no. 6, pp. 391–403, 1998.
39. ADF, "Scm, theoretical chemistry, vrije universiteit, amsterdam, the netherlands."

40. C. L. Donley, J. Zaumseil, J. W. Andreasen, M. M. Nielsen, H. Sirringhaus, R. H. Friend, and J.-S. Kim, "Effects of packing structure on the optoelectronic and charge transport properties in poly (9, 9-di-n-octylfluorene-alt-benzothiadiazole)," *J. Am. Chem. Soc.*, vol. 127, no. 37, pp. 12890–12899, 2005.
41. J. M. Lupton, "Single-molecule spectroscopy for plastic electronics: Materials analysis from the bottom-up," *Adv. Mat.*, vol. 22, no. 15, pp. 1689–1721, 2010.
42. S. Habuchi, H. Fujita, T. Michinobu, and M. Vacha, "Twist angle plays an important role in photophysical properties of a donor–acceptor-type conjugated polymer: A combined ensemble and single-molecule study," *J. Phys. Chem. B*, vol. 115, no. 49, pp. 14404–14415, 2011.
43. J. W. Levell, A. Ruseckas, J. B. Henry, Y. Wang, A. D. Stretton, A. R. Mount, T. H. Galow, and I. D. Samuel, "Fluorescence enhancement by symmetry breaking in a twisted triphenylene derivative," *J. Phys. Chem. A*, vol. 114, no. 51, pp. 13291–13295, 2010.
44. S. Grimme and M. Parac, "Substantial errors from time-dependent density functional theory for the calculation of excited states of large pi systems," *ChemPhysChem*, vol. 4, no. 3, pp. 292–295, 2003.
45. Y.-L. Wang and G.-S. Wu, "Improving the tddft calculation of low-lying excited states for polycyclic aromatic hydrocarbons using the tamm-dancoff approximation," *Int. J. Quant. Chem.*, vol. 108, p. 430, 2007.
46. A. Dreuw, J. L. Weisman, and M. Head-Gordon, "Long-range charge-transfer excited states in time-dependent density functional theory require non-local exchange," *J. Chem. Phys.*, vol. 119, p. 2943, 2003.
47. A. Dreuw and M. Head-Gordon, "Failure of time-dependent density functional theory for long-range charge-transfer excited states: The zincbacteriochlorin-bacteriochlorin and bacteriochlorophyll-spheroidene complexes," *J. Am. Chem. Soc.*, vol. 126, no. 12, pp. 4007–4016, 2004.
48. M. Wanko, M. Garavelli, F. Bernardi, T. A. Niehaus, T. Frauenheim, and M. Elstner, "A global investigation of excited state surfaces within time-dependent density-functional response theory," *J. Chem. Phys.*, vol. 120, pp. 1674–1692, Jan. 2004.
49. A. Pogantsch, G. Heimel, and E. Zojer, "Quantitative prediction of optical excitations in conjugated organic oligomers: A density functional theory study," *J. Chem. Phys.*, vol. 117, p. 5921, 2002.
50. M. J. Peach, P. Benfield, T. Helgaker, and D. J. Tozer, "Excitation energies in density functional theory: An evaluation and a diagnostic test," *J. Chem. Phys.*, vol. 128, p. 044118, 2008.
51. B. M. Wong and T. H. Hsieh, "Optoelectronic and excitonic properties of oligoacenes: substantial improvements from range-separated time-dependent density functional theory," *J. Chem. Theory Comput.*, vol. 6, no. 12, pp. 3704–3712, 2010.
52. R. M. Richard and J. M. Herbert, "Time-dependent density-functional description of the 11 a state in polycyclic aromatic hydrocarbons: Charge-transfer character in disguise?," *J. Chem. Theory Comput.*, vol. 7, no. 5, pp. 1296–1306, 2011.

53. D. Jacquemin, E. A. Perpète, I. Ciofini, and C. Adamo, "Assessment of functionals for td-dft calculations of singlet- triplet transitions," *J. Chem. Theory Comput.*, vol. 6, no. 5, pp. 1532–1537, 2010.
54. J. S. Sears, T. Koerzdoerfer, C.-R. Zhang, and J.-L. Brédas, "Communication: Orbital instabilities and triplet states from time-dependent density functional theory and long-range corrected functionals," *J. Chem. Phys.*, vol. 135, p. 151103, 2011.
55. T. Körzdörfer, J. Sears, C. Sutton, and J.-L. Brédas, "Long-range corrected hybrid functionals for π -conjugated systems: Dependence of the range-separation parameter on conjugation length," *J. Chem. Phys.*, vol. 135, p. 204107, 2011.
56. J. Gierschner, J. Cornil, and H.-J. Egelhaaf, "Optical bandgaps of π -conjugated organic materials at the polymer limit: Experiment and theory," *Adv. Mat.*, vol. 19, no. 2, pp. 173–191, 2007.
57. A. Izmaylov and G. Scuseria, "Why are time-dependent density functional theory excitations in solids equal to band structure energy gaps for semilocal functionals, and how does nonlocal hartree-fock-type exchange introduce," *J. Chem. Phys.*, vol. 129, no. 3, pp. 34101–34101, 2008.